arXiv:1201.3668v2 [hep-ph] 8 Mar 2012

New physics contributions to $A_{FB}^{t\bar{t}}$ at the Tevatron

Sudhansu S. Biswal[1] *, Subhadip Mitra[2] †, Rui Santos[3,4] ‡,
Pankaj Sharma[5] §, Ritesh K. Singh[6] ¶ and Miguel Won[7] **
[1] *Department of Physics, Orissa University of Agriculture and Technology, Bhubaneswar 751003, India.*
[2] *Institute of Physics, Bhubaneswar 751005, India.*
[3] *Instituto Superior de Engenharia de Lisboa,*
Rua Conselheiro Emídio Navarro 1, 1959-007 Lisboa, Portugal.
[4] *Centro de Física Teórica e Computacional,*
Faculdade de Ciências, Universidade de Lisboa,
Av. Prof. Gama Pinto 2, 1649-003 Lisboa, Portugal.
[5] *Physical Research Laboratory, Ahmedabad, India.*
[6] *Department of Physical Sciences, Indian Institute of Science Education and Research – Kolkata,*
Mohanpur campus, 741252, West Bengal, India and
[7] *LIP - Departamento de Física, Universidade de Coimbra, Coimbra, Portugal.*

(Dated: March 9, 2012)

The Tevatron has measured a discrepancy relative to the Standard Model prediction in the forward-backward asymmetry in top quark pair production. This asymmetry grows with the rapidity difference of the two top quarks. It also increases with the invariant mass of the tt pair, reaching, for high invariant masses, 3.4 standard deviations above the Next to Leading Order prediction for the charge asymmetry of QCD. However, perfect agreement between experiment and the Standard Model was found in both total and differential cross section of top quark pair production. As this result could be a sign of new physics we have parametrized this new physics in terms of a complete set of dimension six operators involving the top quark. We have then used a Markov Chain Monte Carlo approach in order to find the best set of parameters that fits the data, using all available data regarding top quark pair production at the Tevatron. We have found that just a very small number of operators are able to fit the data better than the Standard Model.

I. INTRODUCTION

The most recent measurement of the forward-backward asymmetry, $A_{FB}^{t\bar{t}}$, in top quark pair production at the Tevatron [1, 2] was performed by the CDF collaboration using a data sample with 5.3 fb^{-1} of integrated luminosity [3]. After background subtraction, the value of $A_{FB}^{t\bar{t}}$ in the center-of-mass (CM) frame of the top quarks is

$$A_{FB}^{t\bar{t}} = 0.158 \pm 0.074 \tag{1}$$

which constitutes about two standard deviations above the Next-to-Leading-Order (NLO) Standard Model (SM) prediction [4]

$$A_{FB}^{t\bar{t},\mathrm{SM}} = 0.058 \pm 0.009 \quad . \tag{2}$$

Despite the discrepancy in $A_{FB}^{t\bar{t}}$, the total $t\bar{t}$ production cross section is in good agreement with the SM prediction. In fact, with 4.6 fb^{-1} collected luminosity, the top quark pair production cross section [5] yields the result

$$\sigma_{t\bar{t}}^{\mathrm{Measured}} = 7.70 \pm 0.52 \quad pb \tag{3}$$

for a top quark of mass 172.5 GeV, which is in good agreement with the theoretical prediction [6]

$$\sigma_{t\bar{t}}^{\mathrm{SM}}(\mathrm{MCFM}) = 7.45^{+0.72}_{-0.63} \quad \mathrm{pb} \tag{4}$$

* sudhansu.biswal@gmail.com
† smitra@iopb.res.in
‡ rsantos@cii.fc.ul.pt
§ pankajs@prl.res.in
¶ ritesh.singh@iiserkol.ac.in
** miguel.won@coimbra.lip.pt

where MCFM stands for Monte Carlo for FeMtobarn processes [7]. Measurements of the $t\bar{t}$ differential cross section with the $t\bar{t}$ invariant mass ($m_{t\bar{t}}$), $d\sigma/dm_{t\bar{t}}$ were also performed by the CDF collaboration [8]. With an integrated luminosity of 2.7 fb^{-1} CDF has tested the $m_{t\bar{t}}$ spectrum for consistency with the SM. The results are presented in table I. They have concluded that there is no evidence of non-SM physics in $m_{t\bar{t}}$ distributions. Hence, whatever new physics explains the forward-backward asymmetry in $t\bar{t}$ production, it has to comply with all other measurements that are in agreement with the SM. Finally, measurements of the asymmetry for two regions of the top-antitop rapidity difference (ΔY) and for two regions of the invariant mass ($m_{t\bar{t}}$) were performed by the CDF collaboration in [3]. The results are presented in table II together with the theoretical predictions . The asymmetry at high mass is 3.4 standard deviations above the NLO prediction for the charge asymmetry of QCD. Recently the electroweak contributions to the asymmetry were re-analysed [9, 10] just to conclude that the observed mass-dependent forward-backward asymmetry still shows a 3σ deviation in the high mass region. Inclusion of corrections beyond NLO does not change this picture as well [11]. The separate results at high mass and large ΔY contain partially independent information on the asymmetry mechanism. Therefore, a total of 14 observables were measured at the Tevatron. This set of experimental values will be used to investigate whether the complete set of effective dimension six operators is able to describe the possible new physics responsible for the observed discrepancies while retaining the measurements in agreement with the SM. Recently D0 [12] has measured $A_{FB}^{t\bar{t}}$ with 5.4 fb^{-1} of collected luminosity. As discussed in [13], their analysis does not observe a significant rise of the folded detector level asymmetry with respect to $m_{t\bar{t}}-$ and ΔY. Until these results are unfolded they can not be directly compared to the CDF ones, even if at the detector level they appear to be consistent within errors. We did not use the results [12] in our analysis.

Bin (GeV)	σ (CDF result) (pbarn)	σ (SM-NLO) (pbarn)
350-400	3.115 ± 0.559	2.450
400-450	1.690 ± 0.269	1.900
450-500	0.790 ± 0.170	1.150
500-550	0.495 ± 0.114	0.600
550-600	0.285 ± 0.071	0.400
600-700	0.230 ± 0.073	0.310
700-800	0.080 ± 0.037	0.100
800-1400	0.041 ± 0.021	0.036

TABLE I: CDF measurements of $d\sigma/dm_{t\bar{t}}$ [8] (integrated in each bin). We bin-wise scale our SM result (at LO) to match the SM-NLO result to emulate a $m_{t\bar{t}}$ dependent k-factor for fitting. The SM-NLO values are extracted from the plot in [14].

Observables	CDF result	SM prediction
$A_{FB}^{t\bar{t}}(\lvert\Delta Y_t\rvert < 1.0)$	(0.026 ± 0.118)	(0.039 ± 0.006)
$A_{FB}^{t\bar{t}}(\lvert\Delta Y_t\rvert > 1.0)$	(0.611 ± 0.256)	(0.123 ± 0.008)
$A_{FB}^{t}(m_{t\bar{t}}-)$	(-0.116 ± 0.153)	(0.040 ± 0.006)
$A_{FB}^{t}(m_{t\bar{t}}+)$	(0.475 ± 0.114)	(0.088 ± 0.013)

TABLE II: CDF measurements [3] and SM predictions for the Forward-Backward Asymmetry for two regions of ΔY_t and for two regions of $m_{t\bar{t}}$. $A_{FB}^{t}(m_{t\bar{t}}+)$ stands for $A_{FB}^{t\bar{t}}(m_{t\bar{t}} > 450$ GeV), while $A_{FB}^{t}(m_{t\bar{t}}-)$ stands for $A_{FB}^{t\bar{t}}(m_{t\bar{t}} < 450$ GeV).

There have been several attempts to explain this discrepancy. The most popular collection of models among theorists when trying to account for the Tevatron results are the ones with new gauge bosons, and in particular, axigluons, W$'$ and Z$'$ bosons [15]. Explanations in the framework of SuperSymmetric models were discussed in [16]. Other possible justifications for the inconsistency between theory and experiment in the asymmetry, while leaving the cross section for $t\bar{t}$ production within measured uncertainties, include t-channel exchange of color sextet or triplet scalar particles [17], s-channel coloured unparticle contributions [18] or s-channel new colour octet vector bosons contributions [19], light coloured particles from a

particular SU(5) GUT model [20], extra dimensions [21], SO(10) models [22], SO(5) $\otimes$ U(1) gauge-Higgs unification models [23], new heavy quarks [24], diquark models [25] and models where $SU(3)_c$ QCD theory is extended to $SU(N)_c$ which is spontaneously broken at a scale just above the weak scale [26].

The search for resonances decaying into $t\bar{t}$ has also been carried out at the Tevatron [27] (see also [28]) with negative results. CDF has tested vector resonances with masses between 450 GeV and 1500 GeV with widths equal to 1.2 % of their mass. With 4.8 fb^{-1} of integrated luminosity they found no evidence of resonant production of $t\bar{t}$ candidate events. This result sustains the argument of integrating out new heavy fields and strengthens the idea of adopting a model independent approach in explaining the measured asymmetry at the Tevatron. An independent approach, with the recourse to higher dimension operators was already discussed in [29]. In this work we propose to study the effect of dimension six flavour changing neutral current (FCNC) operators together with four fermion (4F) operators. In order to find the best set of parameters that fits the data we will use a Markov Chain Monte Carlo (MCMC) approach.

The paper is organized as follows. The next section is devoted to describe the effective operator approach and the number of independent operators that will be used in the analysis. In section 3 we describe the MCMC method and we present the results for the complete set of operators. Finally a discussion on the results and the conclusions are presented in section 4.

II. THE EFFECTIVE OPERATOR APPROACH

The Standard Model of particle physics is the low energy limit of a more general theory which could manifest itself through a set of effective operators of dimensions higher than four. The effective operator formalism assumes that this more general theory would be visible at very high energies and at an energy scale lower than Λ, the set of higher order operators would be suppressed by powers of Λ. The Lagrangian of the new theory can be written as a series in Λ with operators obeying the gauge symmetries of the SM

$$\mathcal{L} \;=\; \mathcal{L}^{SM} \;+\; \frac{1}{\Lambda}\,\mathcal{L}^{(5)} \;+\; \frac{1}{\Lambda^2}\,\mathcal{L}^{(6)} \;+\; O\left(\frac{1}{\Lambda^3}\right) \quad , \tag{5}$$

where $\mathcal{L}^{SM}$ is the SM lagrangian and $\mathcal{L}^{(5)}$ and $\mathcal{L}^{(6)}$ contain all the dimension five and six operators respectively. This formalism allow us to parametrize new physics, beyond that of the SM, in a model-independent manner. The term $\mathcal{L}^{(5)}$ is eliminated by baryon and lepton number conservation. Thus, any new particle or interaction is hidden in the dimension six operators which are listed in [30, 31].

We divide the dimension six operators in two groups, the four-fermion (4F) operators and the non-4F operators. The later can then be grouped according to the gauge boson present in the triple vertex. As we are discussing $t\bar{t}$ production, the non-4F operators contributing to the process have at least one top quark in the interaction. Operators with one top quark, a light up-quark and one gauge boson will be called FCNC operators. If the gauge boson is a gluon they are classified as strong FCNC operators [32, 33]; otherwise they will be called electroweak FCNC operators [34, 35].

When looking for new physics that would explain the $t\bar{t}$ asymmetry in the framework of the effective operator approach we start by looking at the dimension six non-FCNC operators. As the final state is $t\bar{t}$, the only possible new vertex is an anomalous $gt\bar{t}$ interaction. Its contribution to the process would originate from the diagrams presented in Fig. 1. However, because the initial state is symmetric, these

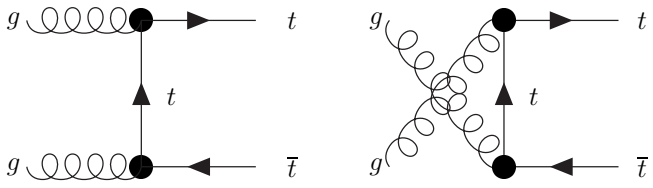


FIG. 1: Feynman diagrams for $t\,\bar{t}$ production via anomalous $gt\bar{t}$ interaction.

diagrams will only contribute to the cross section but not to the asymmetry. Therefore, any changes

produced by these operators would change only the cross section, but not the asymmetry where the discrepancy is. The next class of operators we discuss are the FCNC ones. In this case there are two sets of diagrams to consider: the ones initiated by gluons and the ones initiated by light quarks. For the same

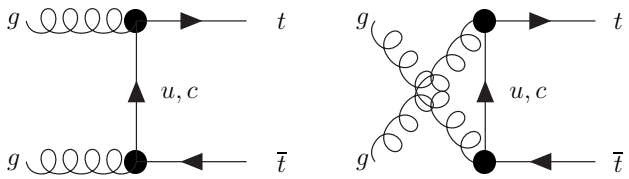


FIG. 2: Feynman diagrams with FCNC operators for $t\,\bar{t}$ production via gluon fusion.

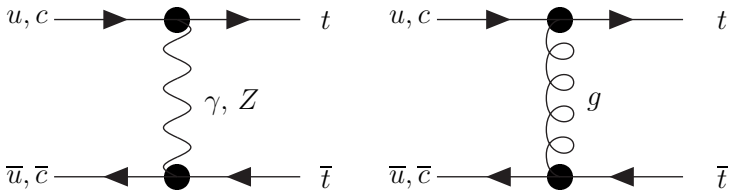


FIG. 3: FCNC Feynman diagrams for $t\,\bar{t}$ production via $q\bar{q}$ fusion.

reasons discussed for Fig. 1 the contribution of the diagrams in Fig. 2 to the asymmetry is negligible. Therefore there are only contributions coming from the diagrams in Fig. 3. Regarding those diagrams (Fig. 3), and taking into account that the contribution of the c-quark is much smaller than that of the u-quark, we discard all contributions that have a c quark in the initial state. Note that there are no s-channel contributions for the FCNC case because we have a top-antitop pair in the final state. Finally we will consider all 4F-fermion operators as shown in Fig. 4. Note that we will consider not only the

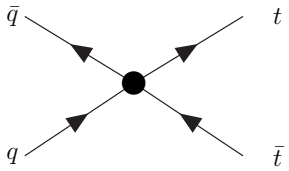


FIG. 4: Four-fermion Feynman diagrams for $t\,\bar{t}$ production.

interference term with the SM contribution, of order $1/\Lambda^2$ but also the modulus-square terms of order $1/\Lambda^4$. We will now discuss the minimum number of operators to be used in our analysis.

A. Effective operators in the strong sector

Following the notation of [30], the operators contributing to the strong FCNC vertices can be written as

$$\mathcal{O}^{ij}_{uG\phi} \,=\, \bar{q}^i_L\,\lambda^a\,\sigma^{\mu\nu}\,u^j_R\,\tilde{\phi}\,G^{a\mu\nu}\,, \tag{6}$$

and

$$\mathcal{O}^{ij}_{uG} \,=\, \bar{u}^i_R\,\lambda^a\,\gamma_\mu D_\nu u^j_R\,G^{a\mu\nu}\,, \quad \mathcal{O}^{ij}_{qG} \,=\, \bar{q}^i_L\,\lambda^a\,\gamma_\mu D_\nu q^j_L\,G^{a\mu\nu}\,, \tag{7}$$

where $G^a_{\mu\nu}$ is the gluonic field tensor, u^i_R stands for a right-handed quark singlet and q^i_L represents the left-handed quark doublet. FCNC occurs because one of the indices is always equal to 3 while the other is

either 1 or 2, that is, there is always one (and one only) top-quark present in the operator; the remaining fermion field in the interaction is either a u or a c-quark. Throughout this section we assume that $\mathcal{O}^{ij}$ and $\mathcal{O}^{ji}$ are independent operators and the hermitian conjugate of all the operators are included in the final Lagrangian. The operators in (6) are related to the operators in (7) through equations of motion that also involve 4F operators [30–33, 36]. However, the 4F operators appearing in those equations have either one or three top-quarks [36]. Therefore, if those 4F operators can be discarded, operators in (7) can be discarded as well. The operators presented in this section will give rise to the FCNC vertices of the form $g\,t\,\bar{u_i}$ (with $u_i = u\,,\,c$) and the corresponding hermitian conjugate interaction with an independent coefficient.

B. Effective operators in the electroweak sector

There are also effective operators stemming from the electroweak sector that would give rise to new FCNC interactions involving the top quark [34, 35]. We start by listing the chirality flipping operators which are the equivalent to the ones in the strong sector, the only difference being the gluonic tensor replaced by the U(1) and SU(2) field tensors. They can be written as

$$\mathcal{O}^{ij}_{uB\phi} \,=\, \bar{q}^i_L\,\sigma^{\mu\nu}\,u^j_R\,\tilde{\phi}\,B_{\mu\nu}\,,\quad \mathcal{O}^{ij}_{uW\phi} \,=\, \bar{q}^i_L\,\tau_I\,\sigma^{\mu\nu}\,u^j_R\,\tilde{\phi}\,W^I_{\mu\nu}\,, \tag{8}$$

and

$$\mathcal{O}^{ij}_{uB} \,=\, \bar{u}^i_R\,\gamma_\mu D_\nu u^j_R\,B^{\mu\nu}\,,\quad \mathcal{O}^{ij}_{qB} \,=\, \bar{q}^i_L\,\gamma_\mu D_\nu q^j_L\,B^{\mu\nu}\,,\quad \mathcal{O}^{ij}_{uW} \,=\, \bar{q}^i_L\,\tau_I\,\gamma_\mu D_\nu\,q^j_L\,W^I_{\mu\nu}\,, \tag{9}$$

where $B^{\mu\nu}$ and $W^I_{\mu\nu}$ are the $U(1)_Y$ and $SU(2)_L$ field tensors, respectively. There are also equations of motion in the electroweak sector that relate the operators in (8) with the ones in (9) and with 4F operators [36]. A similar analysis to the one performed for the strong sector regarding the contribution of the 4F operators leads to the conclusion that we can neglect the operators (9) in our analysis.

Besides chirality-flipping operators there are chirality conserving FCNC operators. Their flavour conserving counterparts are already present in the SM lagrangian at tree-level. In fact, the vertex $\bar{t}tZ$ has two vector contributions of different magnitudes, one proportional to $\gamma_\mu\,\gamma_L$ and the other proportional to $\gamma_\mu\,\gamma_R$. Hence the flavour conserving contribution would modify the Z boson neutral current. All the chirality conserving operators involve the Higgs doublet. As the Higgs field is electrically neutral, there are more effective operators which will only contribute to new Z FCNC interactions. This set of operators can be written as

$$\mathcal{O}^{ij}_{\phi u} \,=\, i\,(\phi^\dagger D_\mu\phi)\,(\bar{u}^i_R\,\gamma^\mu\,u^j_R)\,, \tag{10}$$

$$\mathcal{O}^{(1),ij}_{\phi q} \,=\, i\,(\phi^\dagger D_\mu\phi)\,(\bar{q}^i_L\,\gamma^\mu\,q^j_L)\,,\quad \mathcal{O}^{(3),ij}_{\phi q} \,=\, i\,(\phi^\dagger\,\tau_I\,D_\mu\phi)\,(\bar{q}^i_L\,\gamma^\mu\,\tau_I\,q^j_L)\,, \tag{11}$$

and

$$\mathcal{O}^{ij}_{D_u} \,=\, (\bar{q}^i_L\,D^\mu\,u^j_R)\,D_\mu\tilde{\phi}\,,\quad \mathcal{O}^{ij}_{\bar{D}_u} \,=\, (D^\mu\bar{q}^i_L\,u^j_R)\,D_\mu\tilde{\phi}\,. \tag{12}$$

Again, the use of the equations of motion allow us to discard the operators in (12). In the electroweak sector, there are now 4F operators with one top and one anti-top. However, those 4F operators always have one b-quark in the interaction or, if not, are CKM suppressed making its contribution to the $t\bar{t}$ asymmetry negligible. Furthermore, as was shown in [36], for all the operators in (10) and (11), $\mathcal{O}^{ij}$ and $\mathcal{O}^{ji}$ are not independent. This means that the number of independent operators in (10) and (11) is reduced to three (for each light flavour). Finally, for this particular study, we can group $\mathcal{O}^{(1),ij}_{\phi q}$ and $\mathcal{O}^{(3),ij}_{\phi q}$ under the same Lorentz structure which further reduces the number of independent operators in (11) to two for each light flavour.

The above discussion leads us to the conclusion that the minimum number of operators needed to describe the asymmetry is 8 for each light flavour.

The amplitudes were generated with CalcHEP [37], the Feynman rules for the effective operators were derived with LanHEP [38] and the integration was performed using the CUBA library [39].

C. Four-fermion operators

We now turn to the four-fermion operators. In order to make the analysis as clear as possible we will reduce the operators to a manageable number making use of all allowed reduction procedures, from equations of motion to Fierz identities. Again, because the largest contribution to $t\bar{t}$ production occurs in $u\bar{u}$ fusion, we will discard all non u-quarks contribution in our study. We end up with a total of 12 operators in agreement with [40], that is, 12 operators for each light up-quark flavour and we do not consider operators with down-quarks in the initial state. This simplification allow us to find hints of the type of operators that can contribute to the asymmetry according to the its Lorentz structure. We write the four fermion lagrangian as

$$\begin{aligned}\mathcal{L}_6^{4F} &= \frac{g_s^2}{\Lambda^2}\sum_{A,B}\left[C_{AB}^1(\bar{u}_A\gamma_\mu u_A)(\bar{t}_B\gamma^\mu t_B) + C_{AB}^8(\bar{u}_A T^a\gamma_\mu u_A)(\bar{t}_B T^a\gamma^\mu t_B)\right] + \\ &\frac{g_s^2}{\Lambda^2}\sum_{A\neq B}\left[N_{AB}^1\,(\bar{u}_A\gamma_\mu t_A)(\bar{t}_B\gamma^\mu u_B) + N_{AB}^8\,(\bar{u}_A T^a\gamma_\mu t_A)(\bar{t}_B T^a\gamma^\mu u_B)\right]\end{aligned}$$

where $T^a = \lambda^a/2$, $\{A, B\} = \{L, R\}$, and the exponent 1 and 8 denotes a color singlet and a color octet interaction, respectively.

III. RESULTS

A. Parameter sampling method

In order to find the best set of parameters that fits the data we use a Markov Chain Monte Carlo (MCMC) approach. We start with a random point from the multi-dimensional parameter space for the chosen model. The χ^2 for this point is calculated and a likelihood is assigned to it. This likelihood is a measure of how well a set of data is reproduced for a given point in the model parameter space. Following the notation of [41], this function is defined as

$$\mathbf{G}(O, O_{exp}, \Delta O) = exp\left[\frac{-\chi^2(O, O_{exp}, \Delta O)}{2}\right] \tag{13}$$

where

$$\chi = \frac{O - O_{exp}}{\Delta O} \tag{14}$$

and O is the value of the observable for a given point of parameter space, O_{exp} is the central value of the observable and ΔO is the 1σ error. The absolute value of the likelihood function is irrelevant for our analysis. What is relevant is the ratio of likelihoods, that is, the comparison of the likelihoods of two consecutive points in the chain. We follow the Metropolis-Hastings (MH) algorithm - the Markov chain is started from a random initial value in parameter space with a given likelihood that depends on the constraints imposed by the data set. Next, a new point is generated randomly with a probability distribution centred around the old point and the likelihoods of the two points are compared - if the likelihood of the next point is larger than the one for the current point the next point is appended to the chain, otherwise the current point is replicated in the chain. We have repeated this procedure with 10 different random starting points. We scan with flat priors (i.e. a linear sampling over the parameters) and we have checked that the chains have a very good convergence behaviour. In all calculations of the top production cross sections we use the top mass as the renormalization and factorization scale. We take $m_t = 175$ GeV and to take into account the NLO corrections we have chosen a $k-$factor of 1.41 [6, 7]. Further, we use a bin-wise scaling for the $m_{t\bar{t}}$ distribution to emulate the $m_{t\bar{t}}$ dependent $k-$factor.

Constant	Operator
α_1	$\mathcal{O}^{ut}_{uG\phi}$
α_2	$\mathcal{O}^{tu}_{uG\phi}$
α_3	$\mathcal{O}^{ut}_{uW\phi}$
α_4	$\mathcal{O}^{tu}_{uW\phi}$
α_5	$\mathcal{O}^{ut}_{uB\phi}$
α_6	$\mathcal{O}^{tu}_{uB\phi}$
α_7	$\mathcal{O}^{ut}_{\phi u} + \mathcal{O}^{tu}_{\phi u}$
α_8	$\mathcal{O}^{(3,tu)}_{\phi q} + \mathcal{O}^{(3,ut)}_{\phi q}$

TABLE III: Relation between the constants presented in the plots and the independent FCNC operators in the strong and electroweak sectors.

B. Strong and Electroweak operators

In order to simplify the notation we have replaced the original constants from the operators in the strong and electroweak sectors by α_i with $i = 1, 8$. This correspondence between constants α_i and the operators themselves is presented in table III. As an example, the first operator $\mathcal{O}^{ut}_{uG\phi}$ would appear in the effective Lagrangian as

$$\frac{\alpha^{ut}_{uG\phi}}{\Lambda^2}\,\mathcal{O}^{ut}_{uG\phi} \quad . \tag{15}$$

Considering $\Lambda = 1\ TeV$ then α_1 is defined as

$$\alpha_1 = \frac{\alpha^{ut}_{uG\phi}}{\Lambda^2}\,TeV^2 \tag{16}$$

which renders α_1 dimensionless. Similar definitions hold for the remaining α_i constants. Table III shows the relations between all the constants shown in the plots and the independent FCNC operators in the strong and electroweak sectors.

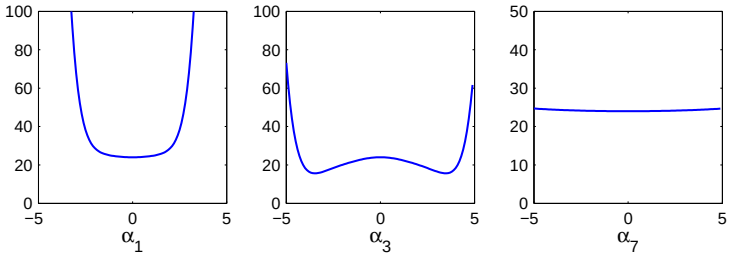


FIG. 5: The χ^2 as a function of α_1, α_3 and α_7 with each parameter taken non-zero at a time. The most favoured values are $\alpha_1 = 0$ and $|\alpha_3| \neq 0$. There are no preferred values for α_7.

We first present our results for the Strong and Electroweak FCNC operators (SEFCNC). In Fig. 5 we present the χ^2 as a function of α_1, α_3 and α_7, keeping only one of the coefficients non-zero at a time. These three curves are representative of the χ^2 distribution behaviour for the complete set of SEFCNC operators. In fact, we can group operators α_1 and α_2 as for both $\alpha_1 = 0$ and $\alpha_2 = 0$ are the most favoured values. The operators that are preferentially non zero when taken one at a time are α_3, α_4, α_5 and α_6. In this case the preferred values are close to $\alpha_i = \pm 4$ (see α_3 in Fig 5). Finally both α_7 and α_8 seem to be completely unconstrained as they have an almost flat χ^2 distribution for the entire α_i range presented. We have then proceeded to scan over the 8 parameters (α_i, $i = 1-8$) using the MCMC method with flat prior as described in the previous section. The range for all parameters was chosen to be $-10 < \alpha_i < 10$. The complete set of 14 experimental observables, presented in the introduction, is used to calculate the χ^2 and hence the likelihood. After the likelihood mapping for the model, we have obtained the one dimensional

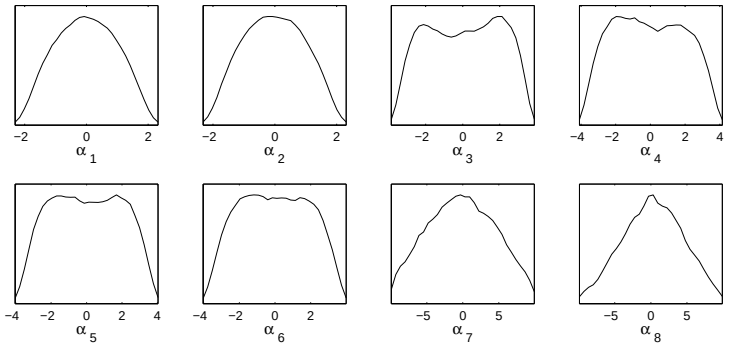


FIG. 6: One dimensional likelihood distribution of the parameters α_1 to α_8 after the fit.

likelihood distribution of the parameters which is presented in Fig 6. It is clear from the figure that both α_1 and α_2, the FCNC operators stemming from the strong sector, are strongly constrained to be in the range -2 to 2. Operators α_3 to α_6, the chirality-flipping FCNC operators coming from the electroweak sector, have to be in the range -4 to 4. Finally the chirality-conserving operators from the electroweak sector, α_7 and α_8 are very mildly constrained and, as we will show later, the center-peaked shape of the distribution is only a reflection of the correlations of these parameters with the constrained ones. In

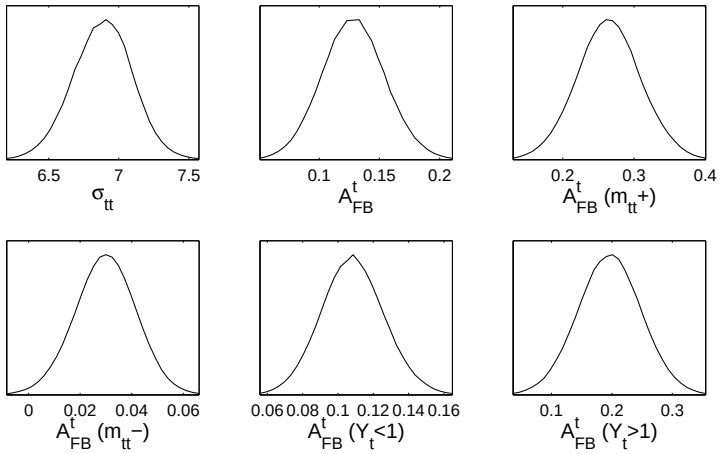


FIG. 7: One dimensional likelihood distribution of the total cross section and all asymmetries after the fit.

order to understand how well the model fits into the experimental observables we present in fig 7 the one dimensional likelihood distribution of the observables after the fit. Considering the central values of the observables presented in the introduction, we conclude that the SEFCNC set of operators prefer a lower value of the cross section while generating suitable values for the total forward-backward asymmetry. The values for $A^t_{FB}(m^+_{tt})$ and $A^t_{FB}(y^+_t)$ are below their experimental central values but well within the error bands. This shows that there is some compromise between the values of the parameters in the attempt to fit all observable simultaneously giving rise to a slight difference between the input observables and the ones originated from the posterior probability distribution functions (pdfs).

We now move to the study of the possible two-dimensional correlation between pairs of parameters. In Fig. 8 we present the two-dimensional correlation plots for the most representative scenarios. It is clear from the figure that there is no correlation between α_1 and α_2. Furthermore, these operators are very strongly constrained. On the other hand, there are several pairs of values that cannot be zero simultaneously. This is the case of (α_3,α_4) – the ones from SU(2), (α_5,α_6) – the ones from U(1) and (α_3,α_5), (α_4,α_6) – these are the U(1) and SU(2) combination where the indices of the operators O^{ij} are the same as for example in $\mathcal{O}^{ut}_{uW\phi}$ and $\mathcal{O}^{ut}_{uB\phi}$. For the pairs ($\alpha_4$,$\alpha_5$) and ($\alpha_3$,$\alpha_6$) the preferred values lie in the region $\alpha_4^2 = \alpha_5^2$ and $\alpha_3^2 = \alpha_6^2$ respectively. This happens to the combination of SU(2) and U(1) operators with the ij indices exchanged. Finally operators α_7 and α_8 do not appear to be much

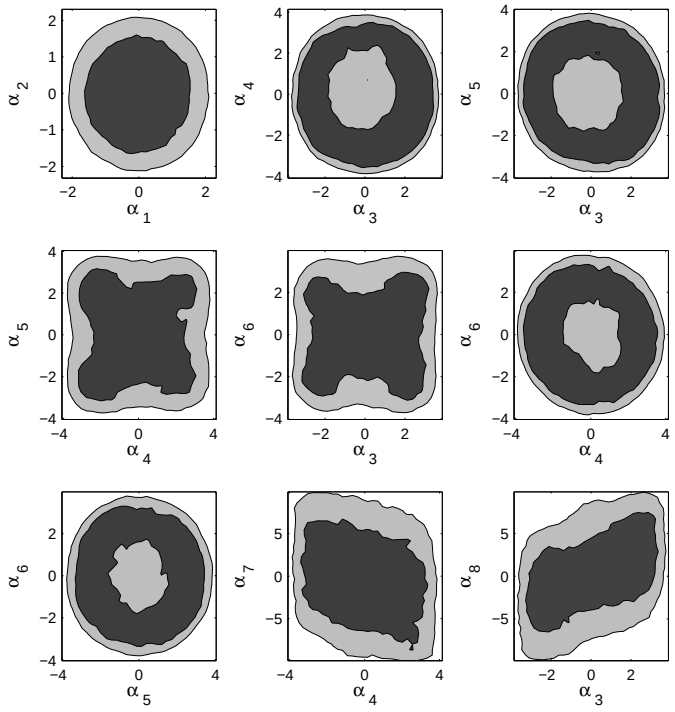


FIG. 8: Two-dimensional correlation plots for the strong and electroweak FCNC parameters. Only the most relevant correlations are shown. The shaded areas are the ones where the values of α_i reach their highest probability - the darker ones represent 95 % CL while the lighter ones are for 68 % CL

constrained when plotted against the remaining operators. There are however mild correlations - if we take for instance the pair (α_4,α_7) it is clear that for $\alpha_4 < 0$, α_7 prefers to be positive and if $\alpha_4 > 0$, α_7 prefers to be negative.

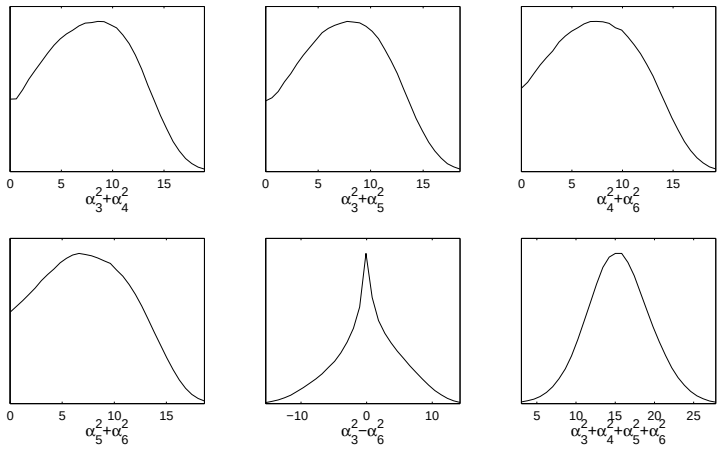


FIG. 9: Likelihood distributions for the most relevant combination of parameters.

With the hints from Fig. 8 about which parameters prefer to be non-zero after the fit, we have tried to understand if one could make a more strong statement about the appearance of new physics related to the Strong and Electroweak dimension six FCNC operators. We note that the contributions of α_7 and α_8 are irrelevant because the change in likelihood is very small when these parameters are varied as shown in figures 5 and 6. On the other hand, α_1 and α_2 can lead to a large change in the likelihood - the preferred points are therefore $\alpha_1 = 0 = \alpha_2$. Hence, we look at the most relevant combinations of the remaining parameters. The likelihood distributions for those combinations are shown in Fig. 9. It is clear

that all the correlated pairs of parameters prefer to be non-zero simultaneously, like for instance (α_3,α_4), which have a peak between 5 and 10. Again, the likelihood plot for $\alpha_3^2 - \alpha_6^2$ peaks at 0 indicating that $\alpha_3^2 = \alpha_6^2$ is the preferred parameter choice as also seen in Fig. 8. However, the most interesting case is the likelihood for $\alpha_3^2 + \alpha_4^2 + \alpha_5^2 + \alpha_6^2$ – in this case we are certain that at least one of the four parameters has to be non-zero in order to fit the data. This is a very strong statement because it means that new physics coming from these operators can help curing the asymmetry discrepancy and in order to solve it at least one of the operators has to be present.

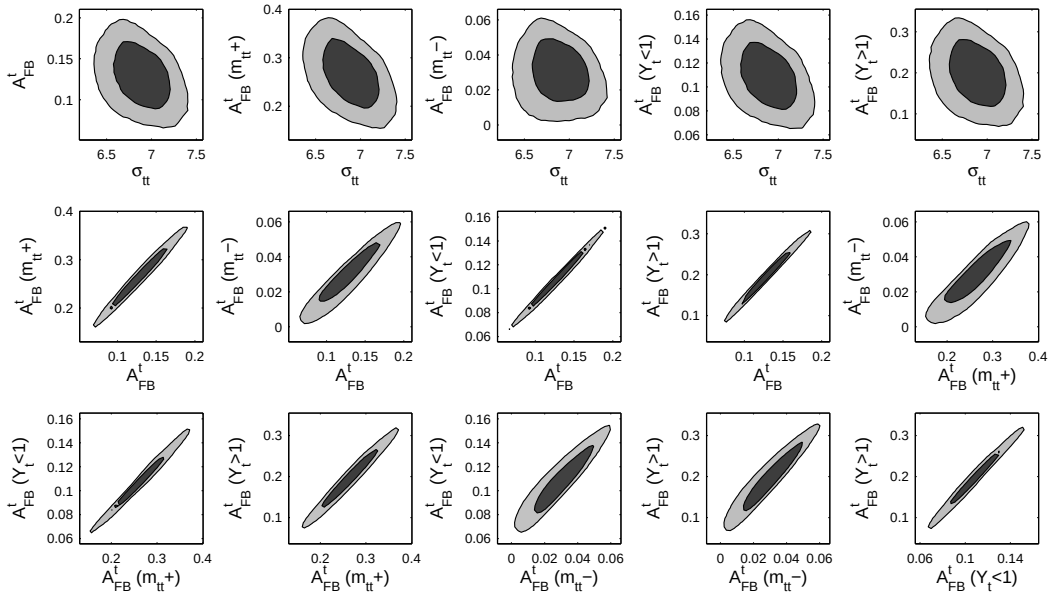


FIG. 10: Two-dimensional correlations between cross sections and asymmetries and between the different asymmetries.

In Fig. 10 we present the two-dimensional correlation between several observables after the fit. In the first row one can see that there is a negative correlation between asymmetries and total cross section. Hence, to get the right asymmetries the cross section moves to its lower preferred value. On the other hand, all asymmetries have positive correlations and are highly correlated – if one of them increases the other increases as well. Therefore, there is a tension between cross sections and asymmetries that reflects the difficulty of fitting all the observables with the set of SEFCNC operators. Nevertheless, a non zero contribution from the operators α_3 to α_6 provides a better fit than the SM one.

In Table. IV, we show the best fit values along with 68% and 95% Bayesian confidence intervals (BCI) for all the parameters and selected observables. The BCIs are derived from the one-dimensional marginalized distributions, as shown in figures 5 and 6, while the best fit point is the one with least $\chi^2 = 14.2$. Thus, the best fit point does not need to be at the center of the marginalized BCIs. For the SM we have $\chi^2 = 24.0$ and it is the sizeable contributions from $\alpha_3, ..., \alpha_6$ operators that lead to the reduction in the χ^2 for our fits. We again note that the combination $\alpha_3^2 + \alpha_4^2 + \alpha_5^2 + \alpha_6^2 > 7.5$ with 97.5% CL, i.e. it is almost certainly non-zero.

We have also listed the posterior BCI for the cross section and the asymmetries in table IV. The best fit value of the total cross section, and also the 95% BCI, are somewhat smaller than the measured central value. The same trend is observed for all the asymmetries except for the integrated asymmetry $A_{FB}^{t\bar{t}}$ which is correctly reproduced and the $A_{FB}^{t}(m_{tt}-)$ asymmetry which is most likely positive in our model. As previously discussed, the reduction of the cross section values and asymmetries is a result of the negative correlations between them.

Quantities	Best fit	68% interval lower	68% interval upper	95% interval lower	95% interval upper
α_1	-0.548	-1.081	1.066	-1.797	1.793
α_2	-0.449	-1.102	1.053	-1.812	1.781
α_3	-2.024	-2.222	2.293	-3.257	3.288
α_4	2.913	-2.327	2.250	-3.443	3.446
α_5	2.403	-2.210	2.254	-3.334	3.379
α_6	0.742	-2.172	2.163	-3.330	3.317
α_7	-3.318	-5.257	4.901	-8.763	8.536
α_8	-3.146	-4.106	4.647	-7.931	8.148
σ_{tt}	6.817	6.670	7.093	6.453	7.299
$A_{FB}^{t\bar{t}}$	0.153	0.102	0.155	0.078	0.181
$A_{FB}^{t}(m_{t\bar{t}}-)$	0.044	0.018	0.041	0.006	0.053
$A_{FB}^{t}(m_{t\bar{t}}+)$	0.310	0.220	0.309	0.177	0.354
$A_{FB}^{t}(Y_t < 1)$	0.126	0.090	0.126	0.074	0.144
$A_{FB}^{t}(Y_t > 1)$	0.245	0.143	0.248	0.093	0.299
$\alpha_3^2+\alpha_4^2+\alpha_5^2+\alpha_6^2$	18.91	11.43	19.39	7.50	23.46

TABLE IV: Best fit values and the Bayesian confidence intervals (BCI) for parameters and the observables.

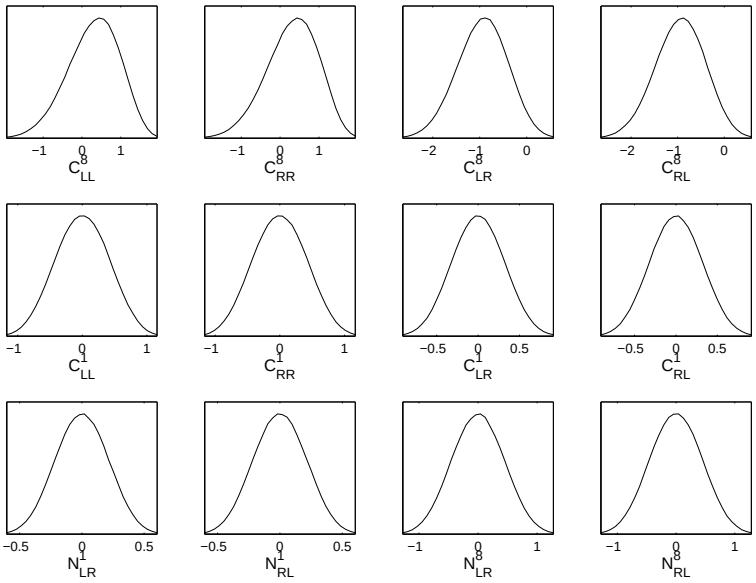


FIG. 11: Likelihood distribution for the parameters of the four-fermion Lagrangian, after the fit.

C. Four fermion operators

We now turn our attention to the four-fermion (4F) effective Lagrangian. We should start by mentioning that recently [42], a complete calculation of the forward-backward asymmetry and of the total cross section of top quark pair production induced by 4F-operators was performed for the Tevatron up to $O(\alpha_s^2/\Lambda^2)$. The results show that next-to-leading order QCD corrections can change both the asymmetry and the total cross section by about 10%. As discussed in section II C, there are a total of 12 independent operators for the study of $t\bar{t}$ production and under the conditions described previously which mainly means we are only considering the u-quark contribution in the initial state. We have scanned linearly over the 12 parameters from the 4F-Lagrangian using the MCMC method. The range chosen for all parameters was again from -10 to 10. In Fig. 11 we present the likelihood distribution for all the 4F

parameters, after the fit. A few comments are in order. First, operators in one row can only interfere with parameters in the same row. Second, only parameters in the first row interfere with the SM Lagrangian and consequently the main contribution for the asymmetry has to come from the parameters presented in the first row. This is clear from the plot as the four distributions in the first row are the only asymmetric ones - all other parameters in the following two rows have not only symmetric distributions but they show that the preferred value of these parameters is zero. However, in the case of 4F operators the

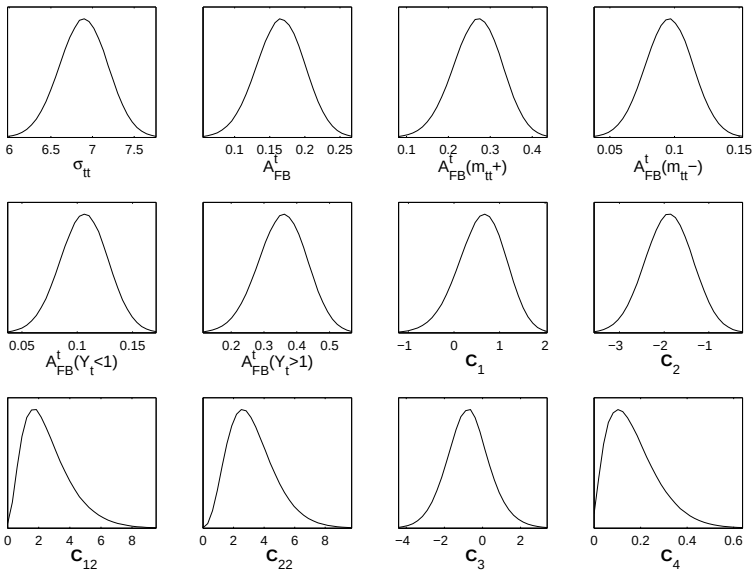


FIG. 12: Likelihood distribution for the total cross section and for the asymmerties and for the six independent combinations of the 4F Lagrangian parameters, after the fit.

cross sections and the asymmetries depend only on six combinations of the parameters. Therefore we have decided to present in Fig. 12 the likelihood distribution for those combinations together with the likelihood distributions of the total cross section and a few selected asymmetries. The relation between the new parameters and the original ones present in the 4F Lagrangian is

$$
\begin{aligned}
C_1 &= C^8_{LL} + C^8_{RR} \\
C_2 &= C^8_{LR} + C^8_{RL} \\
C_{12} &= (C^8_{LL})^2 + (C^8_{RR})^2 + \frac{9}{2}\left[(C^1_{LL})^2 + (C^1_{RR})^2\right] \\
C_{22} &= (C^8_{LR})^2 + (C^8_{RL})^2 + \frac{9}{2}\left[(C^1_{LR})^2 + (C^1_{RL})^2\right] \\
C_3 &= C^8_{LL}C^8_{LR} + C^8_{RR}C^8_{RL} + \frac{9}{2}\left[C^1_{LL}C^1_{LR} + C^1_{RR}C^1_{RL}\right] \\
C_4 &= (N^1_{LR})^2 + (N^1_{RL})^2 + \frac{2}{9}\left[(N^8_{LR})^2 + (N^8_{RL})^2\right] \quad .
\end{aligned}
\tag{17}
$$

It is clear that the experimental observables are well described by the fit. Regarding the parameters, the most relevant fact, that could already be inferred form Fig. 12, is that C_2 prefers to be non-zero and, for the same reason, the likelihood of both C_{12} and C_{22} peaks at 1. A similar trend can now be seen in the two-dimensional correlations presented in Fig. 13. It is clear that at 95 % CL the value zero is excluded in the top right plot. In the top left plot the value zero is still inside the 95 % CL contour. Regarding the correlations between cross section and asymmetries, and between pair of asymmetries, after the fit, the general trend is very similar to the one presented in the previous section for the strong and electroweak FCNC operators. Therefore we will make no further comments on those correlations.

In Fig. 14 we present two dimensional correlations between C_1 and C_2 and the total cross section, total asymmetry and the parameter C_{22}. We see that while C_1 is positively correlated with both the cross section and the asymmetry, C_2 is positively correlated with the cross section but negatively correlated with the asymmetry. Furthermore C_1, C_2 and C_{22} are all negatively correlated with each other. Finally,

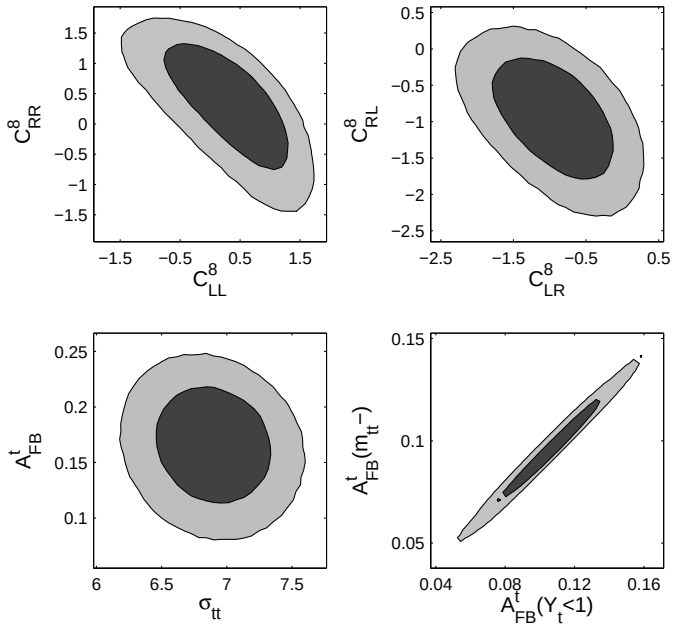


FIG. 13: Two-dimensional correlations between the parameters that can give a significant contribution to the asymmetry. Also shown are typical examples of the correlations between cross section and asymmetries and between two asymmetry observables.

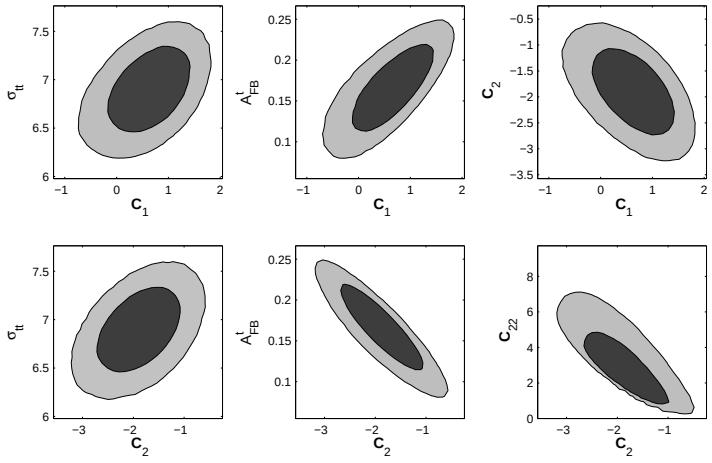


FIG. 14: Two-dimensional correlations between the parameters C_1 and C_2 and the total cross section, total asymmetry and the parameter C_{22}.

we conclude that either C_2, C_{22} or both have to be non-zero which is not surprising given the relations presented in eqs. (3.5).

In Table. V, we show the best fit point along with 68% and 95% BCIs. The best fit point is the one with least $\chi^2 = 6.28$. As seen in figure 13, only C^8_{AB} operators have relevant contributions to both the asymmetries and the cross sections. The weak operators, C^1_{AB} do not interfere with the SM diagrams, contributing therefore more to the cross sections and much less to the asymmetries. Thus, they are strongly constrained through the measured values of the cross sections. The N^i_{AB} operators contribute only to the cross sections and consequently are also strongly constrained and irrelevant as possible new physics contributions.

Again, due to the negative correlations between the cross section and the asymmetries, there is a slight tension in the fits. This leads to a mild preference for lower values of the total cross section. The

		68% interval		95% interval	
Quantities	Best fit	lower	upper	lower	upper
C^8_{LL}	0.915	−0.385	0.968	−1.119	1.466
C^8_{RR}	0.418	−0.368	0.980	−1.104	1.476
C^8_{LR}	−0.934	−1.487	−0.406	−2.031	0.064
C^8_{RL}	−0.963	−1.488	−0.406	−2.035	0.071
C^1_{LL}	−0.136	−0.420	0.420	−0.794	0.792
C^1_{RR}	0.002	−0.422	0.419	−0.795	0.793
C^1_{LR}	−0.082	−0.316	0.316	−0.606	0.606
C^1_{RL}	0.049	−0.316	0.318	−0.606	0.607
N^1_{LR}	0.057	−0.212	0.212	−0.405	0.405
N^1_{RL}	−0.036	−0.212	0.212	−0.405	0.404
N^8_{LR}	0.070	−0.442	0.441	−0.848	0.846
N^8_{RL}	0.040	−0.446	0.443	−0.852	0.850
σ_{tt}	7.054	6.601	7.181	6.315	7.453
$A^{t\bar{t}}_{FB}$	0.191	0.131	0.199	0.096	0.231
$A^t_{FB}(m_{tt}-)$	0.107	0.077	0.114	0.059	0.132
$A^t_{FB}(m_{tt}+)$	0.321	0.211	0.327	0.151	0.379
$A^t_{FB}(Y_t < 1)$	0.121	0.084	0.128	0.063	0.148
$A^t_{FB}(Y_t > 1)$	0.420	0.281	0.430	0.205	0.496

TABLE V: The table of best fit values for the 4F case along with 68% and 95% BCI.

asymmetries, on the other hand, are reasonably well reproduced. We note that, $A^t_{FB}(m_{tt}-)$ prefers to be positive with 4F operators.

IV. BOUNDS ON THE EFFECTIVE OPERATORS

In this section we discuss all possible bounds on the dimension six effective operators described in the previous sections. Our goal is to ascertain whether the values of the couplings multiplying each operator, that could explain the measured asymmetry discrepancy, are still allowed by the available experimental data. We start by considering the dimension six FCNC operators. In section III B we have concluded that only effective operators stemming from the electroweak sector were likely to fit the Tevatron data on the top quark better than the SM. In fact, it is the sizeable contributions from the $\alpha_3, ..., \alpha_6$ operators that lead to the reduction in the χ^2 for our fits. We again note that the combination $\alpha_3^2+\alpha_4^2+\alpha_5^2+\alpha_6^2 > 7.5$ with 97.5% CL, it is almost certainly non-zero. Therefore, we have now to focus on the bounds for operators α_3 to α_6 to understand if such a high value of the constants is not in contradiction with experimental data from other sources.

A very complete analysis on the electroweak FCNC operators was performed in [43] using not only all available data from B physics but also the data from direct FCNC top decays (the later will be updated in this work) [1]. The bounds obtained on the operators taken one at a time are [43] $\alpha_3^2 < 0.81$, $\alpha_4^2 < 0.011$ and $\alpha_6^2 < 0.096$ while the best bound on α_5 was shown to come from the direct constraint on $BR(t \to qZ)$ and $BR(t \to q\gamma)$. Therefore, to satisfy $\alpha_3^2+\alpha_4^2+\alpha_5^2+\alpha_6^2 > 7.5$ one needs $\alpha_5^5 \approx 6.5$. However, such a value of α_5 would imply that $BR(t \to qZ) \approx 3.7\%$ and $BR(t \to q\gamma) \approx 6.3\%$. The most recent direct bounds on $BR(t \to q\gamma)$ and $BR(t \to qZ)$ are the ones from the Tevatron, 3.2% [45] and from the LHC, 1.1% [46], respectively. Hence, it is clear that such high values of α_5 are disallowed by Tevatron and LHC data on the direct searches for FCNC top decays with a photon or a Z-boson in the final state. Furthermore,

[1] Other analysis based on B physics observables and electroweak precision constraints were also performed in [44] leading to similar conclusions.

indirect bounds from HERA, where bounds on cross sections are converted on bounds on the branching ratio, set a limit $BR(t \to q\gamma) \lesssim 0.5\%$ [47]. Also, a combine study on B physics and Tevatron data on top quark production cross section places an indirect bound on the sum of the FCNC branching ratios forcing them to be below the percent level [48]. In conclusion, experimental data from very different sources constrain the operators that could explain the asymmetry in such a way that we consider that it is very unlikely that the observed discrepancy could be explained by these operators.

Contrary to the the dimension six FCNC operators, there are no useful bounds on the four fermion operators involving two top quarks and this is even more so if the top is right-handed. Therefore, only the LHC could place constraints on these operators. However the values of the constants C_i and C_{ij} that could help explain the discrepancy give an extra cross section that is always below 10 pb even for $\sqrt{s} = 14$ TeV. Hence, given the error of $t\bar{t}$ production cross section it is very unlikely that these operators will be constrained in the near future.

V. DISCUSSION AND CONCLUSIONS

In this work we have used a dimension six Lagrangian with FCNC interaction together with four-fermion operators to gain some insight in understanding the discrepancy between the experimental values obtained for the top pair production asymmetry and the corresponding SM predictions. We have build a minimal set of operators and we have used an MCMC approach to find the best simultaneous fit of all independent operators to the available data. Our conclusions regarding which operators give the best fit are as follows

- Strong FCNC operators with coefficients $\alpha_{1,2}$ are most likely close to zero;
- regarding Electroweak FCNC operators with coefficients α_3 to α_6 we conclude that one of them must be non-zero;
- Electroweak FCNC operators with coefficients $\alpha_{7,8}$ are not relevant;
- bounds on electroweak FCNC operators reveal that it is very unlikely that the asymmetry can come from new physics described by these operators;
- Four-fermion operators with coefficients C^8_{AB} contribute to the asymmetries as the ones with coefficients C^1_{AB} give small contributions; the 4F combinations C_1, C_2, C_{12}, C_{22} contribute to the asymmetries;
- Four-fermion operators with coefficients N^i_{AB} contribute to the cross sections only;
- there is in all cases some tension between cross section and asymmetries when a simultaneous fit to all observables is performed;
- the contribution of 4F operators to the cross-section at LHC7 is of the order ± 1.5 pb, which is allowed by the present estimates of the cross-section [49].

It is important to ask how do we figure out which operators are actually responsible for the asymmetry. To that end we note that the asymmetry, although called forward-backward, is actually a C-odd and for CP conserving interaction that can therefore be created by P-odd interactions as well. Further, our operators contribute to the asymmetry in two ways: kinematically and dynamically. The t-channel diagrams with FCNC interaction naturally originate more top quarks in the direction of the incoming u-quark leading to a positive asymmetry as measured by the CDF collaboration. This coupling does not need to be chiral to produce the required asymmetry, although our operators are chiral. For the 4F case, there is no such kinematical asymmetry generation and it is dominantly generated by the unbalance between left and right chiral operators interfering with the SM contribution. Thus, in both cases, we have the presence of chiral interaction, which also incarnates in the form of polarization of the produced top-quark. Hence, a study of such polarization effects [50] as a function of rapidity will be able to provide a probe of possible new physics. Further, our operators are also constrained by the B-physics observables and for simplicity we have not accounted for them in our MCMC. We have nevertheless used the constraints from B-physics to conclude that FCNC operators are unlikely to account for the measured asymmetry at the Tevatron

To conclude, we remark that the $A_{FB}^{t\bar{t}}$observed at CDF can be casted in terms of dimension-six operators and we need more observables, from top-polarization and B-physics, to constrain them due to the multitude of these operators.

Acknowledgments

We thank Rohini Godbole and Saurabh Rindani for useful discussions in the beginning of the collaboration. We also thank the WHEPP-XI organizers for their kind hospitality and for providing a great atmosphere that was the seed of the work presented in this paper. RS is supported in part by the Portuguese *Fundação para a Ciência e a Tecnologia* (FCT) under contract PTDC/FIS/117951/2010, by an FP7 Reintegration Grant, number PERG08-GA-2010-277025 and by PEst-OE/FIS/UI0618/2011. MW is supported by FCT under contract SFRH / BD /45041/2008.

[1] V. M. Abazov *et al.* [D0 Collaboration], Phys. Rev. Lett. **100** (2008) 142002. [arXiv:0712.0851 [hep-ex]].
[2] T. Aaltonen *et al.* [CDF Collaboration], Phys. Rev. Lett. **101** (2008) 202001. [arXiv:0806.2472 [hep-ex]].
[3] T. Aaltonen *et al.* [CDF Collaboration], Phys. Rev. **D83** (2011) 112003. [arXiv:1101.0034 [hep-ex]].
[4] J. H. Kuhn and G. Rodrigo, Phys. Rev. Lett. **81** (1998) 49 [arXiv:hep-ph/9802268]; J. H. Kuhn and G. Rodrigo, Phys. Rev. D **59** (1999) 054017 [arXiv:hep-ph/9807420].
[5] T. Aaltonen *et al.* [CDF Collaboration], Phys. Rev. Lett. **105** (2010) 012001. [arXiv:1004.3224 [hep-ex]].
[6] J. M. Campbell and R. K. Ellis, Phys. Rev. D **60** (1999) 113006 [arXiv:hep-ph/9905386].
[7] Code available from http://mcfm.fnal.gov/ .
[8] T. Aaltonen *et al.* [CDF Collaboration], Phys. Rev. Lett. **102** (2009) 222003 [arXiv:0903.2850 [hep-ex]].
[9] W. Hollik, D. Pagani, [arXiv:1107.2606 [hep-ph]].
[10] J. H. Kuhn, G. Rodrigo, [arXiv:1109.6830 [hep-ph]].
[11] V. Ahrens, A. Ferroglia, M. Neubert, B. D. Pecjak and L. L. Yang, Phys. Rev. D **84** (2011) 074004 [arXiv:1106.6051 [hep-ph]].
[12] V. M. Abazov *et al.* [D0 Collaboration], [arXiv:1107.4995 [hep-ex]].
[13] B. Grinstein, A. L. Kagan, J. Zupan and M. Trott, arXiv:1108.4027 [hep-ph].
[14] Q. -H. Cao, D. McKeen, J. L. Rosner, G. Shaughnessy and C. E. M. Wagner, Phys. Rev. D **81**, 114004 (2010) [arXiv:1003.3461 [hep-ph]].
[15] E. Gabrielli, M. Raidal and A. Racioppi, arXiv:1112.5885 [hep-ph]; E. Gabrielli and M. Raidal, Phys. Rev. D **84** (2011) 054017 [arXiv:1106.4553 [hep-ph]]; J. Cao, K. Hikasa, L. Wang, L. Wu, J. M. Yang, [arXiv:1109.6543 [hep-ph]]; J. A. Aguilar-Saavedra, A. Juste, F. Rubbo, [arXiv:1109.3710 [hep-ph]]; J. -Y. Liu, Y. Tang, Y. -L. Wu, [arXiv:1108.5012 [hep-ph]]; P. Ko, Y. Omura and C. Yu, arXiv:1108.4005 [hep-ph]; S. Jung, A. Pierce, J. D. Wells, [arXiv:1108.1802 [hep-ph]]; Y. Bai, Z. Han, [arXiv:1106.5071 [hep-ph]]; D. Krohn, T. Liu, J. Shelton and L. T. Wang, arXiv:1105.3743 [hep-ph]; C. H. Chen, S. S. C. Law and R. H. C. Li, arXiv:1104.1497 [hep-ph]; J. A. Aguilar-Saavedra and M. Perez-Victoria, Phys. Lett. B **701** (2011) 93 [arXiv:1104.1385 [hep-ph]]; M. R. Buckley, D. Hooper, J. Kopp and E. Neil, Phys. Rev. D **83** (2011) 115013 [arXiv:1103.6035 [hep-ph]]; S. Jung, A. Pierce and J. D. Wells, Phys. Rev. D **83** (2011) 114039 [arXiv:1103.4835 [hep-ph]]; G. Rodrigo and P. Ferrario, Nuovo Cim. C **33** (2010) 04 [arXiv:1007.4328 [hep-ph]]; R. S. Chivukula, E. H. Simmons and C. P. Yuan, Phys. Rev. D **82** (2010) 094009 [arXiv:1007.0260 [hep-ph]]; B. Xiao, Y. k. Wang and S. h. Zhu, Phys. Rev. D **82** (2010) 034026 [arXiv:1006.2510 [hep-ph]]; A. Rajaraman, Z. Surujon and T. M. P. Tait, arXiv:1104.0947 [hep-ph]; J. Shu, K. Wang and G. Zhu, arXiv:1104.0083 [hep-ph]; M. I. Gresham, I. W. Kim and K. M. Zurek, arXiv:1103.3501 [hep-ph]; N. Craig, C. Kilic and M. J. Strassler, arXiv:1103.2127 [hep-ph]; E. R. Barreto, Y. A. Coutinho and J. Sa Borges, Phys. Rev. D **83** (2011) 054006 [arXiv:1103.1266 [hep-ph]]; A. R. Zerwekh, arXiv:1103.0956 [hep-ph]; B. Bhattacherjee, S. S. Biswal and D. Ghosh, arXiv:1102.0545 [hep-ph]; M. I. Gresham, I. W. Kim and K. M. Zurek, arXiv:1102.0018 [hep-ph]; J. Cao, L. Wang, L. Wu and J. M. Yang, arXiv:1101.4456 [hep-ph]; P. H. Frampton, J. Shu and K. Wang, Phys. Lett. B **683** (2010) 294 [arXiv:0911.2955 [hep-ph]]; K. Cheung, W. Y. Keung and T. C. Yuan, Phys. Lett. B **682** (2009) 287 [arXiv:0908.2589 [hep-ph]]; S. Jung, H. Murayama, A. Pierce and J. D. Wells, Phys. Rev. D **81** (2010) 015004 [arXiv:0907.4112 [hep-ph]]; D. K. Ghosh, A. Nyffeler, V. Ravindran, N. Agarwal, P. Agarwal, P. Bandyopadhyay, R. Basu and B. Bhattacherjee *et al.*, Pramana **76**, 707 (2011).
[16] G. Isidori and J. F. Kamenik, arXiv:1103.0016 [hep-ph] J. Cao, Z. Heng, L. Wu and J. M. Yang, Phys. Rev. D **81** (2010) 014016 [arXiv:0912.1447 [hep-ph]].
[17] J. Shu, T. M. P. Tait and K. Wang, Phys. Rev. D **81** (2010) 034012 [arXiv:0911.3237 [hep-ph]].
[18] C. H. Chen, G. Cvetic and C. S. Kim, Phys. Lett. B **694** (2011) 393 [arXiv:1009.4165 [hep-ph]].

[19] H. Wang, Y. k. Wang, B. Xiao and S. h. Zhu, arXiv:1107.5769 [hep-ph]; B. Xiao, Y. k. Wang and S. h. Zhu, arXiv:1011.0152 [hep-ph]; M. V. Martynov and A. D. Smirnov, arXiv:1010.5649 [hep-ph]; M. V. Martynov and A. D. Smirnov, Mod. Phys. Lett. A **25** (2010) 2637 [arXiv:1006.4246 [hep-ph]]; P. Ferrario and G. Rodrigo, Phys. Rev. D **80** (2009) 051701 [arXiv:0906.5541 [hep-ph]].

[20] I. Dorsner, S. Fajfer, J. F. Kamenik and N. Kosnik, Phys. Rev. D **81** (2010) 055009 [arXiv:0912.0972 [hep-ph]].

[21] A. Djouadi, G. Moreau and F. Richard, Phys. Lett. B **701** (2011) 458 [arXiv:1105.3158 [hep-ph]]; M. Bauer, F. Goertz, U. Haisch, T. Pfoh and S. Westhoff, JHEP **1011** (2010) 039 [arXiv:1008.0742 [hep-ph]]; A. Djouadi, G. Moreau, F. Richard and R. K. Singh, Phys. Rev. D **82** (2010) 071702 [arXiv:0906.0604 [hep-ph]]; A. Djouadi, G. Moreau and F. Richard, Nucl. Phys. B **773** (2007) 43 [arXiv:hep-ph/0610173].

[22] K. M. Patel and P. Sharma, JHEP **1104** (2011) 085 [arXiv:1102.4736 [hep-ph]].

[23] N. Uekusa, arXiv:0912.1218 [hep-ph].

[24] H. Davoudiasl, T. McElmurry, A. Soni, [arXiv:1108.1173 [hep-ph]].

[25] A. Arhrib, R. Benbrik and C. H. Chen, Phys. Rev. D **82** (2010) 034034 [arXiv:0911.4875 [hep-ph]].

[26] R. Foot, Phys. Rev. **D83** (2011) 114013. [arXiv:1103.1940 [hep-ph]].

[27] T. Aaltonen *et al.* [The CDF Collaboration], [arXiv:1107.5063 [hep-ex]].

[28] T. Aaltonen *et al.* [CDF Collaboration], [arXiv:1108.4755 [hep-ex]].

[29] J. A. Aguilar-Saavedra, M. Perez-Victoria, [arXiv:1107.2120 [hep-ph]]; J. A. Aguilar-Saavedra, M. Perez-Victoria, [arXiv:1107.0841 [hep-ph]]; J. A. Aguilar-Saavedra, M. Perez-Victoria, [arXiv:1105.4606 [hep-ph]]; J. A. Aguilar-Saavedra, M. Perez-Victoria, JHEP **1105** (2011) 034. [arXiv:1103.2765 [hep-ph]]; C. Delaunay, O. Gedalia, Y. Hochberg, G. Perez and Y. Soreq, arXiv:1103.2297 [hep-ph]; C. Degrande, J. M. Gerard, C. Grojean, F. Maltoni and G. Servant, JHEP **1103** (2011) 125 [arXiv:1010.6304 [hep-ph]]; D. W. Jung, P. Ko, J. S. Lee and S. h. Nam, Phys. Lett. B **691** (2010) 238 [arXiv:0912.1105 [hep-ph]].

[30] W. Buchmüller and D. Wyler, *Nucl. Phys.* **B268** (1986) 621.

[31] B. Grzadkowski, M. Iskrzynski, M. Misiak, J. Rosiek, JHEP **1010** (2010) 085. [arXiv:1008.4884 [hep-ph]].

[32] P. M. Ferreira, O. Oliveira and R. Santos, Phys. Rev. D **73** (2006) 034011 [arXiv:hep-ph/0510087].

[33] P. M. Ferreira and R. Santos, Phys. Rev. D **73** (2006) 054025 [arXiv:hep-ph/0601078].

[34] P. M. Ferreira, R. B. Guedes and R. Santos, Phys. Rev. D **77** (2008) 114008 [arXiv:0802.2075 [hep-ph]].

[35] R. A. Coimbra, P. M. Ferreira, R. B. Guedes, O. Oliveira, A. Onofre, R. Santos and M. Won, Phys. Rev. D **79** (2009) 014006 [arXiv:0811.1743 [hep-ph]].

[36] J. A. Aguilar-Saavedra, Nucl. Phys. **B812**, 181-204 (2009). [arXiv:0811.3842 [hep-ph]].

[37] A. Pukhov *et al.*, arXiv:hep-ph/9908288; A. Pukhov, arXiv:hep-ph/0412191.

[38] A. Semenov, Comput. Phys. Commun. **115** (1998) 124; A. Semenov, Comput. Phys. Commun. **180** (2009) 431 [arXiv:0805.0555 [hep-ph]].

[39] T. Hahn, Comput. Phys. Commun. **168** (2005) 78 [arXiv:hep-ph/0404043].

[40] J. A. Aguilar-Saavedra, Nucl. Phys. **B843** (2011) 638-672. [arXiv:1008.3562 [hep-ph]].

[41] G. Belanger, F. Boudjema, A. Pukhov and R. K. Singh, JHEP **0911** (2009) 026 [arXiv:0906.5048 [hep-ph]].

[42] D. Y. Shao, C. S. Li, J. Wang, J. Gao, H. Zhang, H. X. Zhu, [arXiv:1107.4012 [hep-ph]].

[43] P. J. Fox, Z. Ligeti, M. Papucci, G. Perez and M. D. Schwartz, Phys. Rev. D **78**, 054008 (2008) [arXiv:0704.1482 [hep-ph]].

[44] J. Drobnak, S. Fajfer and J. F. Kamenik, Phys. Lett. B **701** (2011) 234 [arXiv:1102.4347 [hep-ph]]; B. Grzadkowski and M. Misiak, Phys. Rev. D **78**, 077501 (2008) [Erratum-ibid. D **84**, 059903 (2011)] [arXiv:0802.1413 [hep-ph]]; Q. -H. Cao, J. Wudka and C. -P. Yuan, Phys. Lett. B **658** (2007) 50 [arXiv:0704.2809 [hep-ph]]; C. Zhang, N. Greiner and S. Willenbrock, arXiv:1201.6670 [hep-ph];
N. Greiner, S. Willenbrock and C. Zhang, Phys. Lett. B **704**, 218 (2011) [arXiv:1104.3122 [hep-ph]].

[45] F. Abe *et al.* [CDF Collaboration], Phys. Rev. Lett. **80** (1998) 2525.

[46] ATLAS Collaboration, ATLAS-CONF-2011-154 (2011).

[47] H. Abramowicz *et al.* [ZEUS Collaboration], Phys. Lett. B **708** (2012) 27 [arXiv:1111.3901 [hep-ex]].

[48] P. M. Ferreira and R. Santos, Phys. Rev. D **80** (2009) 114006 [arXiv:0903.4470 [hep-ph]].

[49] T. J. Kim, arXiv:1201.4772 [hep-ex].

[50] D. Choudhury, R. M. Godbole, S. D. Rindani and P. Saha, Phys. Rev. D **84**, 014023 (2011) [arXiv:1012.4750 [hep-ph]]; J. Cao, L. Wu and J. M. Yang, Phys. Rev. D **83**, 034024 (2011) [arXiv:1011.5564 [hep-ph]]; D. -W. Jung, P. Ko and J. S. Lee, Phys. Lett. B **701**, 248 (2011) [arXiv:1011.5976 [hep-ph]];

[51] M. I. Gresham, I. -W. Kim and K. M. Zurek, Phys. Rev. D **85**, 014022 (2012) [arXiv:1107.4364 [hep-ph]].